Impaired Cleavage of Preproinsulin Signal Peptide Linked to Autosomal-Dominant Diabetes

Ming Liu,[1,2] Roberto Lara-Lemus,[1] Shu-ou Shan,[3] Jordan Wright,[1] Leena Haataja,[1] Fabrizio Barbetti,[4] Huan Guo,[1] Dennis Larkin,[1] and Peter Arvan[1]

Recently, missense mutations upstream of preproinsulin's signal peptide (SP) cleavage site were reported to cause mutant *INS* gene-induced diabetes of youth (MIDY). Our objective was to understand the molecular pathogenesis using metabolic labeling and assays of proinsulin export and insulin and C-peptide production to examine the earliest events of insulin biosynthesis, highlighting molecular mechanisms underlying β-cell failure plus a novel strategy that might ameliorate the MIDY syndrome. We find that whereas preproinsulin-A(SP23)S is efficiently cleaved, producing authentic proinsulin and insulin, preproinsulin-A(SP24)D is inefficiently cleaved at an improper site, producing two subpopulations of molecules. Both show impaired oxidative folding and are retained in the endoplasmic reticulum (ER). Preproinsulin-A(SP24)D also blocks ER exit of coexpressed wild-type proinsulin, accounting for its dominant-negative behavior. Upon increased expression of ER–oxidoreductin-1, preproinsulin-A(SP24)D remains blocked but oxidative folding of wild-type proinsulin improves, accelerating its ER export and increasing wild-type insulin production. We conclude that the efficiency of SP cleavage is linked to the oxidation of (pre)proinsulin. In turn, impaired (pre)proinsulin oxidation affects ER export of the mutant as well as that of coexpressed wild-type proinsulin. Improving oxidative folding of wild-type proinsulin may provide a feasible way to rescue insulin production in patients with MIDY. ***Diabetes*** **61:828–837, 2012**

Among the many monogenic causes of diabetes (1–3), mutant insulin gene syndrome was originally used to describe three autosomal-dominant mutations associated with an adult-onset, type 2 diabetes-like phenotype (4). More recently, in addition to recessive *INS* gene mutations (5), new *INS* gene mutations have been found to underlie a syndrome we call mutant *INS* gene-induced diabetes of youth (MIDY), in which heterozygotes develop autosomal-dominant diabetes, with onset from neonatal life to adulthood (6–15). The MIDY mutations cause misfolding of the insulin precursor protein (16,17), resulting in retention within the endoplasmic reticulum (ER) of β-cells (18,19). Importantly, such misfolded proinsulin forms protein complexes that can incorporate innocent bystander proinsulin (20), impairing the ER exit of wild-type (WT) proinsulin and decreasing insulin production (21). Moreover, recent studies indicate that insulin deficiency precedes a net loss of β-cell mass (22,23), suggesting that this dominant-negative blockade caused by mutants is sufficient to account for initial onset of diabetes in MIDY (24,25).

In β-cells, insulin synthesis begins with the precursor preproinsulin, which must undergo cotranslational translocation into the ER, signal peptide (SP) cleavage and downstream proinsulin folding. These earliest events are critical to insulin biosynthesis, but they are relatively understudied since the discovery of preproinsulin (26). Two preproinsulin SP mutations located at or next to the SP cleavage site have been recently reported to cause human diabetes (2,3,6,8), which makes investigation of these earliest events especially timely. One of them, preproinsulin-A(SP24)D, was reported to impair preproinsulin processing (26) and induce ER stress; yet, A(SP24)D reportedly produced no significant adverse effect on insulin production from a coexpressed WT allele (27). Thus, it is uncertain why A(SP24)D should not be a recessive rather than a dominant mutation causing severe, early onset, insulin-deficient diabetes.

In this report, we have more closely examined A(SP23)S and A(SP24)D, both reportedly associated with human MIDY (6,7,10,12). We find that A(SP23)S has no detectable biological defect and is likely to be a polymorphic variant. By contrast, upon translocation into the ER lumen, A(SP24)D exhibits defective SP cleavage, resulting in abnormal oxidative folding of downstream proinsulin, forming disulfide-linked protein complexes that are retained in the ER. We demonstrate that A(SP24)D expression results in dominant-negative blockade of coexpressed proinsulin-WT, a common mechanism in MIDY (20,24,25). Finally, we have explored a potential therapeutic mechanism that, in the presence of A(SP24)D, can improve the native oxidative maturation of coexpressed proinsulin-WT, enhancing its export and increasing insulin production.

RESEARCH DESIGN AND METHODS

Materials. Guinea pig anti-porcine insulin, rat insulin (#RI-13 K), and human insulin-specific (#HI-14 K) and proinsulin-specific radioimmunoassay (#HPI-15 K) were from Millipore; rabbit anti-Myc and anti-GFP were from Immunology Consultants Laboratories; Zysorbin was from Zymed; ^{35}S-amino acid mixture (Met+Cys) and pure ^{35}S-Met were from ICN; dithiothreitol (DTT), protein A-agarose, digitonin, *N*-ethylmaleimide (NEM), and radioimmunoassay (RIA)-grade bovine serum albumin were from Sigma-Aldrich; Met/Cys-deficient Dulbecco's modified Eagle's medium (DMEM) and all other tissue culture reagents were from Invitrogen. Plasmids encoding human Ero1α and Ero1β were from Dr. P. Scherer (University of Texas Southwestern), and mouse protein disulfide isomerase (PDI) was from Dr. M. Green (St. Louis University).
Human and mouse preproinsulin mutagenesis. The human *INS* cDNA and mouse *Ins2* cDNA with or without Myc tag as described (21) were subcloned into pTarget and pCMS-GFP vectors. Mutations were introduced using the QuikChange site-directed mutagenesis kit (Stratagene) and confirmed by direct DNA sequencing.

From the [1]Division of Metabolism, Endocrinology & Diabetes, University of Michigan Medical Center, Ann Arbor, Michigan; [2]Tianjin Medical University General Hospital, Tianjin, China; the [3]Division of Chemistry and Chemical Engineering, California Institute of Technology, Pasadena, California; and the [4]Laboratory of Molecular Endocrinology and Metabolism, Bambino Gesù Children's Hospital, Scientific Institute (Istituto Di Ricovero e Cura a Carattere Scientifico), Rome, Italy.
Corresponding authors: Ming Liu, mingli@umich.edu, and Peter Arvan, parvan@umich.edu.
Received 24 June 2011 and accepted 19 December 2011.
DOI: 10.2337/db11-0878

Cell culture, transfection, metabolic labeling, immunoprecipitation, SDS-PAGE, Western blotting, and ER stress response. INS1 (rat) cells, Min6 (mouse) cells, or 293T (human) cells were plated onto 12-well plates 1 day before transfection with Lipofectamine (Invitrogen) using 1 to 2 μg plasmid DNA. At 48 h after transfection, cells were pulse-labeled with ^{35}S-Met/Cys or pure ^{35}S-Met and chased as indicated. Cells used for analysis of (pre)proinsulin oxidative folding were preincubated with 20 mmol/L NEM in PBS on ice for 10 min before lysis. Lysis buffer (1% Triton X-100, 0.1% SDS, Tris, pH 7.4) contained 2 mmol/L NEM and a proteinase inhibitor cocktail. For immunoprecipitation, samples were precleared with Zysorbin and immunoprecipitated as described previously (21). Nonreducing or reducing Tris-Tricine urea–SDS-PAGE was performed as described (18). For Western blotting, 20 μg total lysate protein was boiled in SDS sample buffer with or without 100 mmol/L DTT, resolved by 4–12% NuPage, electrotransferred to nitrocellulose, and blotted with rabbit anti-Myc followed by anti-rabbit–HRP conjugate, with development by enhanced chemiluminescence. The BiP promoter-driven firefly luciferase assay for Min6 cells 48 h posttransfection to express human preproinsulin-WT or mutants (normalized to *Renilla luciferase* activity) was performed as described (21) using the dual-luciferase reporter kit (Promega).

Partial permeabilization of plasma membranes with digitonin. After labeling with ^{35}S-Cys/Met, 293T cells transfected with human preproinsulin-WT or mutant were washed, resuspended, and incubated in 50 μl of 150 mmol/L NaCl, 2 mmol/L $CaCl_2$, 50 mmol/L HEPES, pH 7.5, ± 0.01% digitonin on ice for 10 min. The cells were spun at 14,000 rpm for 10 min at 4°C; the supernate was transferred to a new tube containing 450 μL lysis buffer and the pellet lysed in 500 μL lysis buffer. Both supernate and pellet were immunoprecipitated with anti-insulin or anti-GFP and analyzed using 4–12% NuPage.

Radioimmunoassay of WT human proinsulin and insulin. 293T cells were cotransfected with human preproinsulin-WT and either mouse preproinsulin-WT or mutants, plus empty vector or a vector expressing PDI or ER–oxidoreductin-1 (ERO1), at a DNA molar ratio of 1:2:3. At 40 h posttransfection, medium-bathing transfected cells were collected for an additional 16 h and used to measure secreted human proinsulin using the human proinsulin-specific RIA.

Min6 cells were transfected with vectors expressing human preproinsulin-WT or mutants. At 40 h posttransfection, cells were incubated with DMEM containing 25.5 mmol/L glucose and 10% FBS for 16 h. The media were then collected and cells lysed with acid/ethanol (20) and human insulin measured by human insulin-specific RIA. In parallel, duplicate wells of each transfection were used for isolating total RNA. Human insulin mRNA levels were determined by RT-PCR using forward primer: 5′-GAACCAACACCTGTGCGGCTCAC-3′ and reverse primer: 5′-CGAGGCTTCTTCTACACACCCA-3′. In this way, human insulin protein level was normalized to human insulin mRNA level.

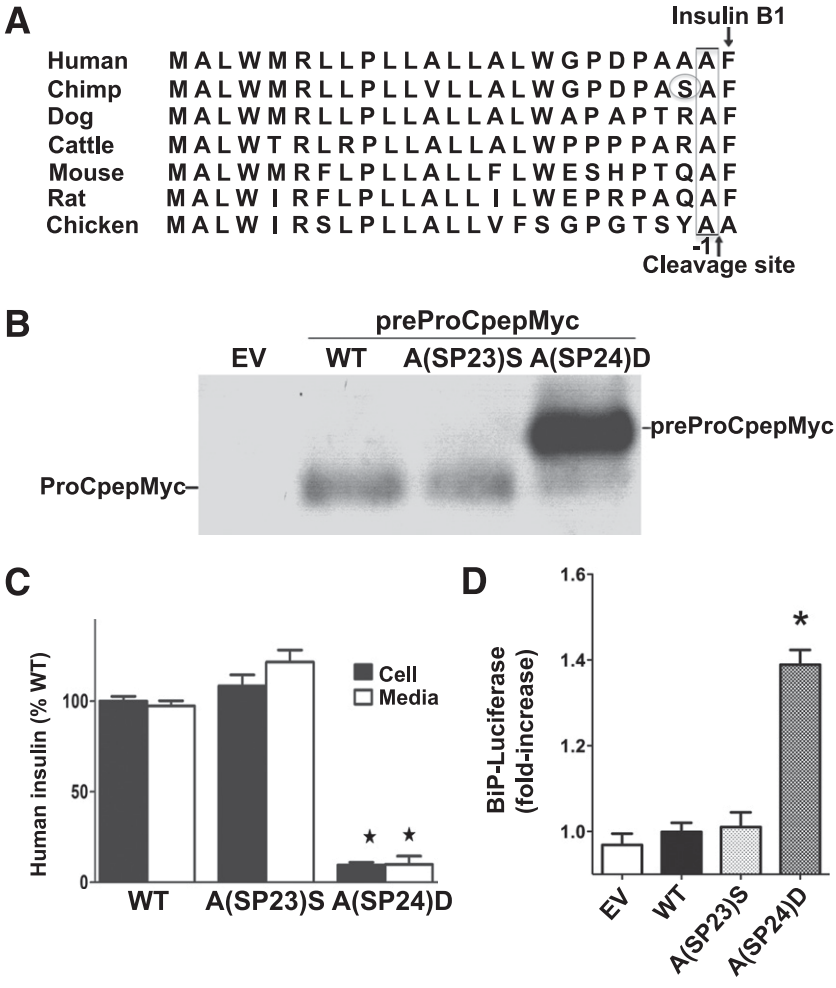

FIG. 1. A(SP23)S exhibits no abnormal phenotype, whereas A(SP24)D exhibits a defect in SP cleavage and insulin production and induces ER stress in β-cells. *A*: Signal sequence alignment of preproinsulins of various species. The arrow indicates the predicted signal peptide cleavage site; the −1 residue is boxed and a Ser-SP23 (−2) residue in chimpanzee preproinsulin is circled. *B*: MIN6 cells were transiently transfected with plasmids encoding hProCpepMyc-WT, A(SP23)S, or A(SP24)D and lysed after 48 h posttransfection, and 20 μg total protein was used for anti-Myc Western blot as described in RESEARCH DESIGN AND METHODS. *C*: MIN6 cells were transiently transfected with human preproinsulin-WT, A(SP23)S, or A(SP24)D plasmids. At 40 h posttransfection, the cells were incubated with fresh DMEM medium containing 25.5 mmol/L glucose and 10% FBS for additional 16 h; the media were collected and cells lysed as in RESEARCH DESIGN AND METHODS. Human insulin in the lysates (black bars) and media (white bars) were quantified using human-specific insulin RIA normalized to human-specific insulin mRNA (a measure of the efficiency of insulin production from the transfected translation product). Results shown are mean values ± SD from three independent experiments. *$P < 0.01$ compared with preproinsulin-WT or A(SP23)S. *D*: Min6 cells cotransfected to express BiP promoter-firefly luciferase, CMV promoter-driven *R. luciferase*, and preproinsulin-WT or mutants were lysed at 48 h posttransfection, and the ratio of firefly/*R. luciferase* was measured. Cells expressing WT proinsulin or empty vector (EV) served as a negative control. Results are expressed as mean ± SD from three independent experiments. *$P < 0.05$ compared with preproinsulin-WT.

Statistical analysis. Statistical analyses were carried out by ANOVA followed by Bonferroni multiple comparison test using GraphPad Prism 5. Data are presented as means ± SD. A P value of <0.05 was taken as statistically significant.

RESULTS

SP cleavage of human preproinsulin-A(SP23)S and A(SP24)D. Evolutionarily, the preproinsulin SP diverges more in sequence than does the insulin B-chain or A-chain (28). In tetrapods, residue A(SP24) predominates at the cleavage site (residue "−1"), whereas there is considerable natural variation at the penultimate "−2" position (Fig. 1*A*). In chimpanzee, S(SP23) predominates (Fig. 1*A*), and there is a polymorphic variation in this position even within the human genome (29). Thus, it was of interest to further investigate the physiological significance of both A(SP23)S and A(SP24)D substitutions.

In MIN6 pancreatic β-cells transfected to express Myc-tagged human preproinsulin [preProCpepMyc (21)], A(SP24)D was predominantly uncleaved, with a minor cleaved band migrating near ProCpepMyc-WT (Fig. 1*B*). Impaired efficiency of SP cleavage (Fig. 1*B*) can directly account for decreased human insulin production (Fig. 1*C*). By contrast, A(SP23)S showed no defect of SP cleavage or human insulin production (Fig. 1*B* and *C*). Moreover, A(SP24)D induced ER stress in Min6 cells, whereas the ER stress response for A(SP23)S was similar to that for preproinsulin-WT (Fig. 1*D*). In 293T cells, newly synthesized A(SP23)S was rapidly processed to proinsulin and secreted, exactly like WT, whereas A(SP24)D showed little preproinsulin processing or secretion (Fig. 2*A*). From multiple such experiments, ≤10% of A(SP24)D underwent SP cleavage (Fig. 2*B*). We examined the subsequent fate of newly synthesized mutant preproinsulin for up to 4 h of chase. Although secretion of either uncleaved or SP-cleaved A(SP24)D was negligible, there was intracellular loss of A(SP24)D, some of which was clearly blocked by the proteasome inhibitor MG132 (Fig. 2*C*). Although the data suggest ER-associated degradation (ERAD) of A(SP24)D at steady state, A(SP24)D showed substantial accumulation in β-cells (Fig. 1*B*). Thus, A(SP23)S exhibits no defect of SP cleavage or insulin production, whereas A(SP24)D exhibits impaired SP cleavage, intracellular retention, at least partial ERAD, activation of ER stress response, and blocked insulin production.

Translocation of preproinsulin-A(SP24)D across the ER membrane. Conceivably, failed SP cleavage could reflect failure of preproinsulin translocation across the ER membrane (30). We used digitonin to partially permeabilize the plasma membrane while keeping organelle membranes intact (31) in cells coexpressing recombinant preproinsulin and cytosolic green fluorescent protein (GFP); upon permeabilization and centrifugation, >50% of cytosolic GFP was relocated from pellet to supernate, whereas both WT and A(SP24)D remained exclusively in the pellet (Fig. 3*A*). Thus, A(SP24)D is not free in the cytosol, implying its association with the ER. It is known that the preproinsulin SP plus the first 14 residues of proinsulin B-chain are sufficient to direct the downstream translation product into the ER lumen (32). To confirm that this is the case for A(SP24)D, we engineered the A(Cpep18)N substitution into the C-peptide (Fig. 3*B*, *top*) to create an artificial *N*-linked glycosylation site that can be used to establish that at least 76 residues of nascent preproinsulin polypeptide have accessed the luminal side of the ER. When combined with the fact that human proinsulin has no methionine residues (i.e., pure ^{35}S-Met can label only preproinsulin; ^{35}S-proinsulin labeling requires ^{35}S-Cys), we found that essentially all molecules of both proinsulin-WT (^{35}S-Cys/Met) and A(SP24)D (either ^{35}S-Met or ^{35}S-Cys/Met) became available in the ER lumen, as established by *N*-linked glycosylation that could be deglycosylated with PNGase F (Fig. 3*B*). Thus, essentially all molecules of A(SP24)D undergo ER translocation.

Disulfide bonding within uncleaved preproinsulin. To our knowledge, no studies have previously examined the relationship between SP cleavage and oxidative folding of

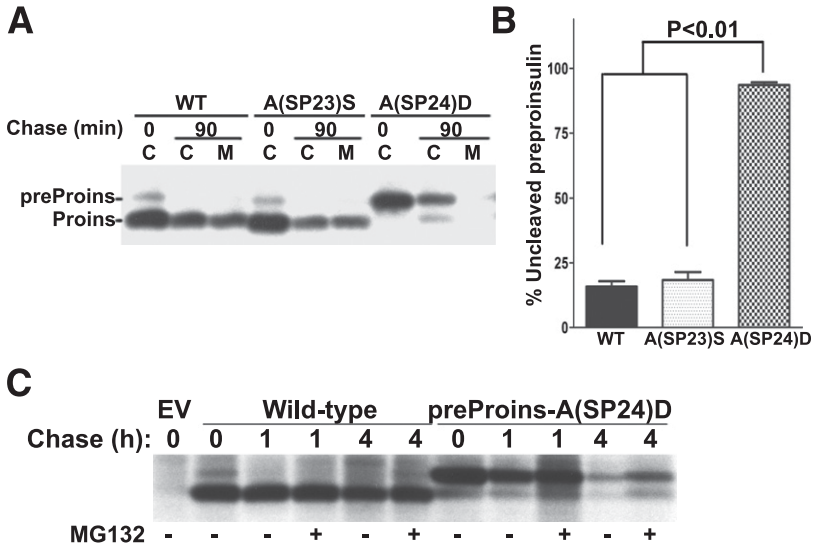

FIG. 2. SP cleavage and ER export of A(SP23)S and A(SP24)D. *A*: Transfected 293T expressing human preproinsulin-WT or mutants were pulse-labeled with ^{35}S-Cys/Met for 10 min followed by 0 or 90 min chase. Cell lysates (C) and chase media (M) were immunoprecipitated with anti-insulin and analyzed using 4–12% NuPage under reducing conditions. *B*: From repeat experiments like that shown in *A*, without chase, the uncleaved and processed preproinsulin bands were quantified by scanning densitometry (± SD). $P < 0.01$ compared to either WT or A(SP23)S. *C*: Transfected 293T cells expressing WT or A(SP24)D were pulse-labeled with ^{35}S-Cys/Met for 30 min followed by 0, 1, or 4 h chase with or without 10 μmol/L MG132. The cell lysates and chase media were combined and immunoprecipitated with anti-insulin and analyzed using 4–12% NuPage under reducing conditions.

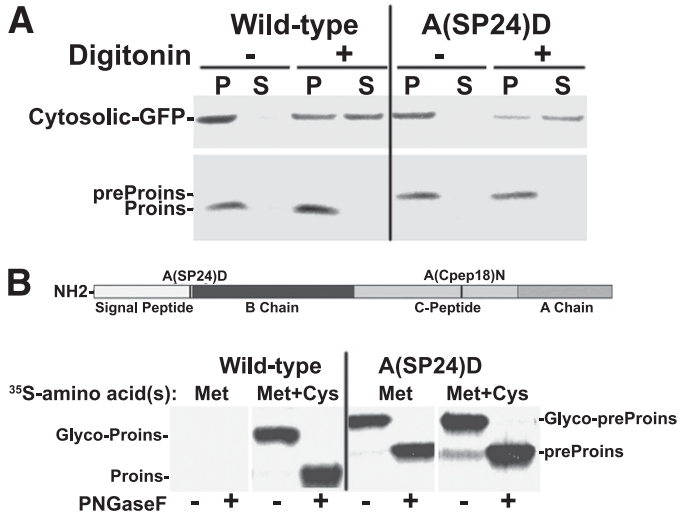

FIG. 3. Translocation of preproinsulin-A(SP24)D across the ER membrane. *A*: At 40 h posttransfection, 293T cells coexpressing cytosolic GFP and preproinsulin-WT or -A(SP24)D were pulse-labeled with ^{35}S-Cys/Met for 15 min and then treated with 0.01% digitonin on ice for 10 min to permeabilize the plasma membrane, which liberates a major fraction of cytosolic GFP. Cells were then sedimented at 14,000 rpm at 4°C for 10 min and each pellet (P) and supernate (S) analyzed sequentially by anti-insulin and anti-GFP immunoprecipitation, 4–12% NuPage, under reducing conditions and autoradiography. *B*: The 18th residue of human preproinsulin C-peptide was mutated from Ala to Asn to create an *N*-linked glycosylation site. At 40 h posttransfection, 293T cells expressing human preproinsulin-A(Cpep18)N bearing or lacking the A(SP24)D mutation were pulse-labeled with either pure ^{35}S-Met or mixed ^{35}S-Cys/Met for 15 min before lysis and immunoprecipitation with anti-insulin. Immunoprecipitates were split in half and either digested (+) or mock digested (−) with PNGase F at 37°C for 1 h before analysis by 4–12% NuPage under reducing conditions. At this exposure, preproinsulin-WT is not detected with pure ^{35}S-Met, indicating that the vast majority of molecules have already undergone SP cleavage; thus, the same sample labeled with ^{35}S-Cys/Met indicates glycosylated (Glyco-Proins) or deglycosylated proinsulin (Proins). However, A(SP24)D remains labeled with pure ^{35}S-Met, indicating the positions of glycosylated (Glyco-preProins) or deglycosylated preproinsulins (preProins).

preproinsulin within the ER. We used nonreducing Tris-Tricine urea–SDS-PAGE (16) to examine disulfide bond formation in recombinant newly synthesized preproinsulin. Uncleaved preproinsulin-WT (labeled with ^{35}S-Met) appears fully reduced (Fig. 4*A*, *lane 2*). Upon SP removal, proinsulin-WT (labeled with ^{35}S-Cys/Met) may begin as a fully reduced species (Fig. 4*A*, *lane 1*, arrow) but proceeds to native and isomeric oxidized proinsulin (lower bands). Within 10 min, reduced (pre)proinsulin nearly vanished, and oxidized native proinsulin became enriched (Fig. 4*B*, *lane 2*), indicating both rapid SP cleavage and downstream proinsulin folding.

For A(SP24)D, the sequence of early events appeared altered: newly synthesized preproinsulin-A(SP24)D (^{35}S-Met–labeled) started to become oxidized (Fig. 4*A*, *lanes 7* and *8*), and this increased after 10 min (Fig. 4*B*, *lane 8*). By comparing the recovery of fully reduced preproinsulin-A(SP24)D by nonreducing gel versus total preproinsulin recovered under reducing conditions, we calculated (from multiple experiments) that 42 ± 2.7% of preproinsulin-A(SP24)D had oxidized (either properly or improperly, see below) at the zero chase time. The oxidized fraction of preproinsulin-A(SP24)D was 61% by 10 min of chase; 86% by 30 min of chase; and 90% under steady-state conditions by Western blotting (Fig. 4*C*, *right*). By contrast, proinsulin-WT was >90% oxidized at the zero chase time, and there was essentially no fully reduced proinsulin-WT remaining after 10 min (Fig. 4*B*). Under steady-state conditions, ≤10% oxidized A(SP24)D remains as monomer recovered under nonreducing conditions (Fig. 4*C*, compare *lanes 3* and *4*), indicating that the majority forms disulfide-linked protein complexes. Most importantly, in β-cells, A(SP24)D coimmunoprecipitated coexpressed proinsulin-WT, which was detected only under reducing conditions; thus, this proinsulin-WT must also have been recruited into disulfide-linked complexes (Fig. 4*D*). Altogether, the data in Figs. 3 and 4 establish that impaired SP cleavage triggers defective oxidative folding within the ER, leaving exposed thiols on preproinsulin that could create cellular problems by participating in inappropriate intermolecular thiol attack.

Inappropriate SP cleavage of preproinsulin-A(SP24)D and dominant-negative blockade of proinsulin-WT. Using the SignalP-3.0 computer-based algorithm, we noted that whereas human preproinsulin-WT uses the AAA-proinsulin sequence to generate proinsulin beginning with the appropriate F(B1) residue, the A(SP24)D sequence predicts SP cleavage at low efficiency, generating a minor portion of AD-Proins that includes two extra residues preceding the proinsulin B-chain (Fig. 5*A*). We therefore designed three additional preproinsulin mutants (AAAAD-Proins, AAAMD-Proins, and AMAD-Proins) intended to interrogate the location of the preproinsulin cleavage site while finding a high-efficiency means to generate the aberrant AD-Proins cleavage product (Fig. 5*A*). By SDS-PAGE/autoradiography after metabolic labeling with ^{35}S-Cys/Met, unlike the inefficient SP cleavage of A(SP24)D (Fig. 5*B*, *lanes 3* and *4*), other bioengineered preproinsulins underwent efficient (but aberrant) SP cleavage. In Fig. 5*B*, a comparison of *lanes 2*, *4*, *6*, *8*, and *10* (each including ^{35}S-Cys label) showed the presence of a cleaved band in every instance. However, when comparing *lanes 3*, *5*, and *7* (Fig. 5*B*) labeled with pure ^{35}S-Met, the cleaved band became undetectable except in *lane 7* (AAAMD-Proins), when methionine was still found to be contained within the product that must have been cleaved upstream of the Met residue. By contrast, in *lane 9* (AMAD-Proins; Fig. 5*B*) the cleaved product had lost the Met residue (i.e., a cleavage site less than three residues upstream from the normal site but containing at least two residues from the normal site). These observations precisely match the cleavage sites predicted. Regardless of whether the cleavage reaction occurred at low efficiency or high efficiency, the aberrant proinsulins bearing two extra NH_2-terminal amino acids in every instance failed to be secreted normally (Fig. 5*C*). Thus, fidelity of SP cleavage, exposing the critical proinsulin NH_2-terminal arm, including phenylalanine-B1 (33), is crucial to normal proinsulin folding and export from the ER.

Because A(SP24)D forms aberrant disulfide-linked protein complexes (Fig. 4*C*) that include coexpressed proinsulin-WT (Fig. 4*D*), we made A(SP24)D-DelCys (in which all six cysteines were mutated) to test for dominant-negative behavior. Interestingly, most of the blockade of WT proinsulin secretion was lost when thiols were eliminated from the A(SP24)D mutant (Fig. 6*A*). These data support the concept of thiol attack as a mechanism of dominant-negative behavior of A(SP24)D (i.e., precisely the danger mechanism that has been proposed for MIDY) (21,25).

Heterozygous patients bearing *INS* gene mutations that cause decreased insulin biosynthesis from the mutant allele

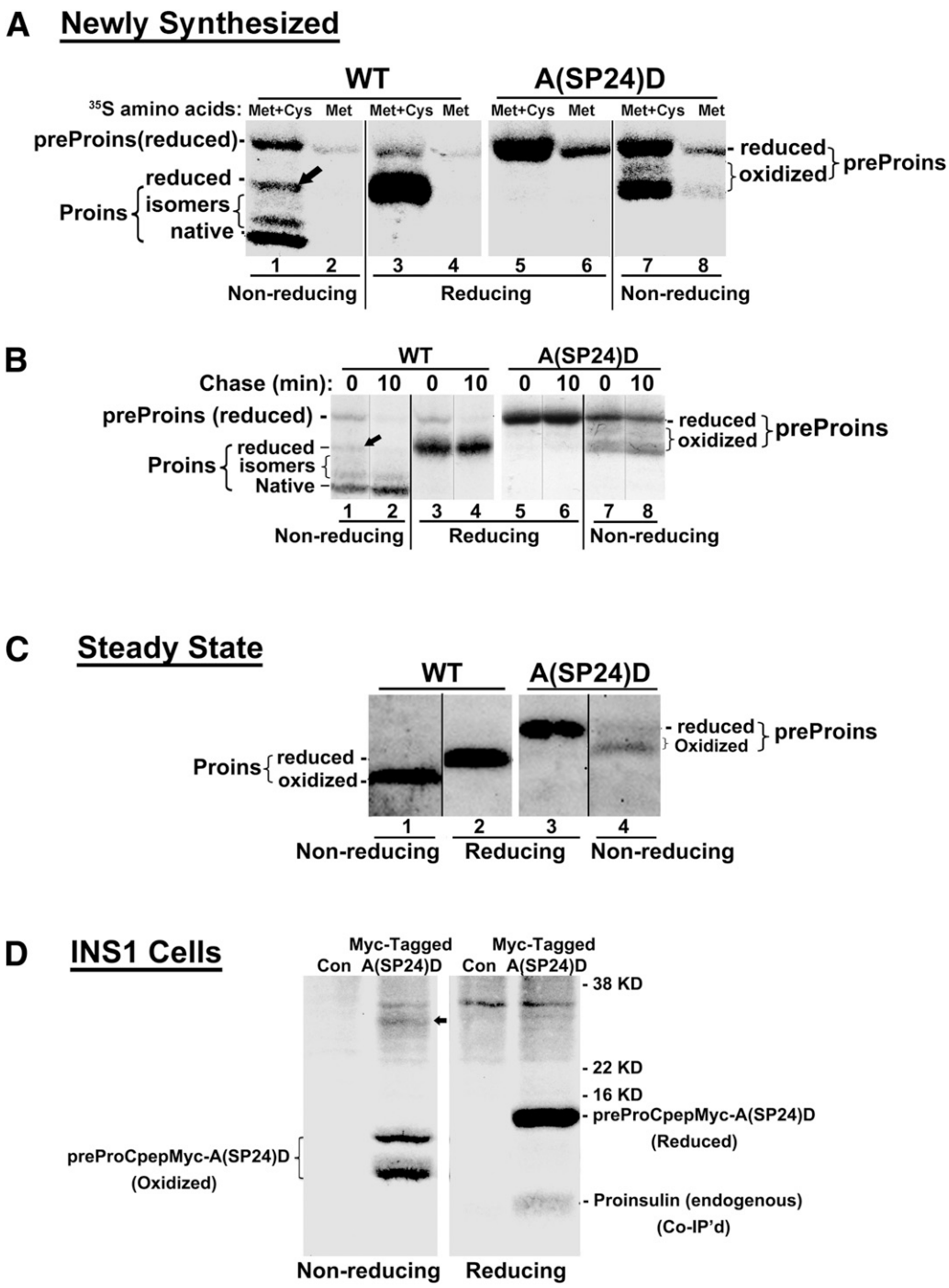

FIG. 4. The kinetics of SP cleavage and disulfide bond formation. *A*: At 40 h posttransfection, 293T cells expressing human preproinsulin-WT or -A(SP24)D were pulse-labeled for 10 min with either ^{35}S-Cys/Met or pure ^{35}S-Met, as indicated. The cells were pretreated with 20 mmol/L NEM in PBS on ice for 10 min before lysis and immunoprecipitation with anti-insulin. The immunoprecipitates were analyzed using Tris-Tricine urea–SDS-PAGE under nonreducing and reducing conditions, as indicated. The positions of both oxidized and reduced forms of preproinsulin (preProins) and proinsulin (Proins) are indicated. *B*: At 40 h posttransfection, 293T cells expressing human preproinsulin WT or A(SP24)D were pulse-labeled with ^{35}S-Cys/Met for 10 min and chased for 0 or 10 min. Newly synthesized preproinsulin (preProins) and proinsulin (Proins) were analyzed as in *A*. *C*: 293T cells transiently transfected to express preProCpepMyc-WT or the same construct bearing A(SP24)D were lysed at 48 h post-transfection, and 20 μg total proteins was resolved by 4–12% NuPage under nonreducing and reducing conditions, as indicated, followed by anti-Myc Western blotting as described in RESEARCH DESIGN AND METHODS. *D*: INS1 cells transfected with preProCpepMyc-A(SP24)D were pulse-labeled with ^{35}S-Cys/Met for 30 min. The cells were lysed and immunoprecipitated with anti-Myc and analyzed as in *A*.

do not develop diabetes (5). Thus, decreased insulin production from A(SP24)D itself cannot account for diabetes in heterozygous patients. To explore this further, individually epitope-tagged and preproinsulin partners were coexpressed in β-cells. A preProCpepMyc construct, either bearing or not bearing the A(SP24)D mutation, was coexpressed in INS1 cells along with preProCpepGFP, a reporter of WT proinsulin trafficking and processing (20,24). Although new synthesis of preProCpepGFP was unaffected by coexpression of A(SP24)D, the production of mature

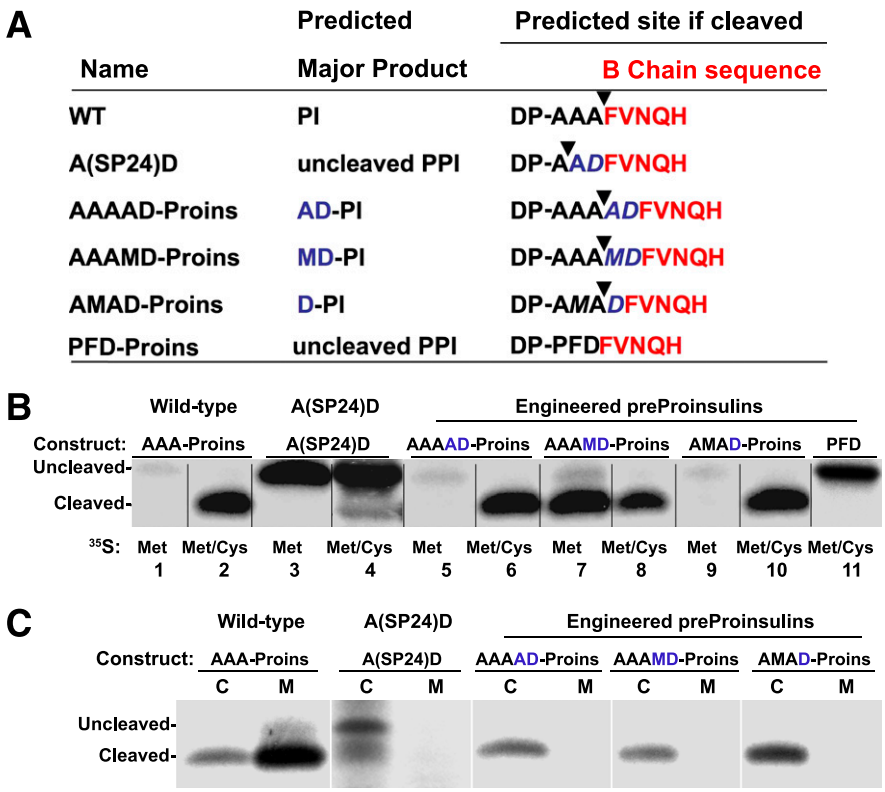

FIG. 5. Inappropriate SP cleavage of A(SP24)D and engineered preproinsulins. *A*: WT or engineered human preproinsulins (with the names indicated in the column at left) show predicted SP cleavage sites are based on the SignalP 3.0 algorithm (http://www.cbs.dtu.dk/services/SignalP/). SP cleavage (black arrowheads) leaves predicted additional residues attached to the NH_2 terminus of the proinsulin B-chain. *B*: At 48 h post-transfection, 293T cells expressing human preproinsulin-WT (AAA-Proins in this panel) or mutants as indicated were pulse-labeled for 15 min with either pure ^{35}S-Met or ^{35}S-Met/Cys as indicated. Cell lysates were immunoprecipitated with anti-insulin and analyzed using 4–12% NuPage under reducing conditions, followed by autoradiography. *C*: Transfected 293T cells were labeled with ^{35}S-Met/Cys for 15 min and chased for 150 min. The cell lysates (C) and chase media (M) were immunoprecipitated and analyzed as in *B*. (A high-quality color representation of this figure is available in the online issue.)

human insulin, as measured by accumulation of the processed CpepGFP over 20 h of continuous metabolic labeling, was clearly inhibited upon coexpression of the mutant (Fig. 6*B*). These data link mutant A(SP24)D expression to insulin deficiency derived from the WT proinsulin allele.

Whereas the AAAAD-Proins construct exclusively forms miscleaved AD-Proinsulin (Fig. 5), we also engineered a preproinsulin (PFD-Proins, Fig. 5*A*) that cannot be cleaved at all by signal peptidase as measured either by pulse-labeling (Fig. 5*B*, *lane 11*) or at steady state (Fig. 6*C*). Individually, these two constructs should be able to test the relative dominant-negative contributions derived from the actual A(SP24)D mutant which, after 1–4 h chase, can be detected as both forms (Fig. 2*C*).

First, to test whether miscleaved AD-Proins was a potent dominant-negative, we coexpressed progressively decreasing doses of AAAAD-Proins with bystander pre-ProCpepMyc-WT to emulate the small quantities of AD-Proinsulin typically synthesized from A(SP24)D. At all expression levels, untagged AD-Proinsulin itself was impaired in the secretory pathway, but only at the highest expression levels did AD-Proinsulin inhibit export of coexpressed bystander ProCpepMyc-WT (Fig. 6*D*, *top*). However, at low expression levels [all of which are higher than that generated from A(SP24)D], AD-Proinsulin could no longer block secretion of ProCpepMyc-WT (Fig. 6*D*, *bottom*).

Next, we found that newly synthesized PFD-Proins also could not be secreted; but more importantly, uncleaved PFD-Proins efficiently blocked in trans the ER export of coexpressed proinsulin-WT (Fig. 6*E*). Thus, PFD-Proins completely emulated the dominant-negative effects of A(SP24)D. Taken together, the data in Fig. 6 strongly suggest that it is the improperly oxidized full-length preproinsulin-A(SP24)D, and not the miscleaved AD-Proins product derived from A(SP24)D, that is primarily responsible for dominant-negative blockade of coexpressed proinsulin-WT in patients with MIDY.

Partial rescue of proinsulin-WT from dominant-negative blockade of A(SP24)D. We have previously demonstrated that MIDY mutants selectively interfere with the oxidative folding to the native state of innocent bystander proinsulin-WT molecules, and promote their ERAD (21). We reasoned that conditions accelerating native disulfide bond formation in proinsulin-WT might help these molecules escape blockade caused by A(SP24)D (and other MIDY mutants). Recent reports indicate that members of the ERO1 family promote formation of proinsulin disulfide bonds (34,35). We therefore explored whether overexpression of ERO1 [or PDI (36)] could help to rescue human proinsulin-WT from blockade by either mouse *Akita* proinsulin [another MIDY mutant (20,21)] or mouse preproinsulin-A(SP24)D. Using a human-proinsulin specific RIA, we found that increased expression of ERO1 (either α or β), but not PDI, showed rescue activity for export of proinsulin-WT (Fig. 7*A*). To confirm this rescue effect in β-cells, we coexpressed human preproinsulin-WT with mouse preproinsulin-A(SP24)D, which lowered the human insulin content of transfected INS1 cells by >70%

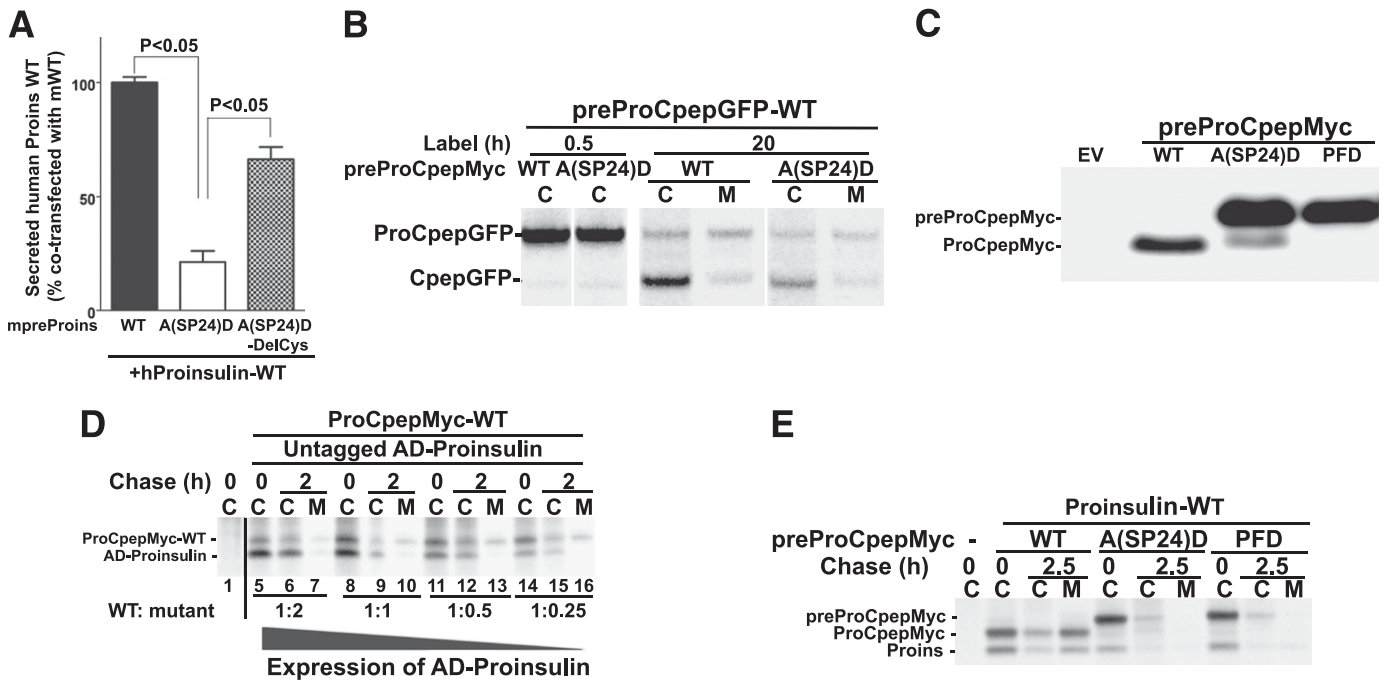

FIG. 6. Dominant-negative blockade of proinsulin-WT caused by preproinsulin-A(SP24)D, miscleaved proinsulin, and uncleaved preproinsulin. *A*: 293T cells were cotransfected to express human preproins-WT with either mouse preproins-WT, A(SP24)D, or A(SP24)D-DelCys [in which all cysteines of A(SP24)D were mutated (21)] at a DNA ratio of 1:2. Beginning at 30 h posttransfection, cells were incubated with DMEM containing 25.5 mmol/L glucose plus 10% FBS for additional 16 h. Media were collected, and a human proinsulin-specific RIA was used to measure secretion of coexpressed human proinsulin-WT. The secretion of human proinsulin coexpressed with mouse preproins-WT served as a positive control (i.e., set to 100%). Results are shown as mean ± SD from three independent experiments. *B*: INS1 cells cotransfected with preProCpepGFP-WT with either preProCpepMyc-WT or A(SP24)D (at a DNA molar ratio of 1:2) were labeled for either 0.5 or 20 h as indicated. The cell lysates (C) and media (M) were immunoprecipitated with anti-GFP and analyzed under reducing conditions. *C*: INS1 cells transfected to express preProCpepMyc-WT, A(SP24)D, or PFD were lysed at 48 h posttransfection. The cell lysates were resolved by 4–12% NuPage under reducing conditions. The proteins were electrotransferred to nitrocellulose and immunoblotted with anti-Myc antibody. *D*: 293T cells cotransfected with preProCpepMyc-WT and untagged AAAAD-Proins (processed to AD-Proins; see Fig. 5*A*) at a range of DNA ratios (indicated below) were pulse-labeled with ^{35}S-Cys/Met for 30 min and chased for 0 or 2 h. Cell lysates (C) and collected chase media (M) were immunoprecipitated with anti-insulin and analyzed under reducing conditions. *E*: 293T cells cotransfected with untagged preproinsulin-WT (processed to Proins) and preProCpepMyc-WT, A(SP24)D, or PFD were pulse-labeled with ^{35}S-Cys/Met for 30 min and chased for 0 or 3 h. Cell lysates (C) and collected chase media (M) were analyzed as in *D*.

(Fig. 7*B*). However, in cells with simultaneously increased expression of ERO1α or ERO1β, human insulin content doubled (Fig. 7*B*). To independently validate these RIA results, we performed pulse-chase experiments like those shown in Fig. 6*E*. Once again, A(SP24)D blocked in trans the export of coexpressed proinsulin-WT (Fig. 7*C*, *lane 7*). However, in cells with increased expression of ERO1α, the behavior of A(SP24)D itself was unaffected, whereas export of coexpressed proinsulin-WT was partially rescued (Fig. 7*C*, *lane 13*). Similar results were obtained upon increased expression of ERO1β (not shown).

To explore further the mechanism of ERO1-mediated rescue of proinsulin-WT, we examined the recovery of the native disulfide isoform of newly synthesized proinsulin-WT relative to total proinsulin-WT recovery under reducing conditions (21). In the presence of A(SP24)D, the oxidative maturation of proinsulin-WT to the native state was significantly decreased (Fig. 8*A*, open bars). However, upon increased expression of ERO1β, the recovery of native disulfide-bonded proinsulin-WT was restored despite the presence of coexpressed A(SP24)D (Fig. 8*A*, *far right black bar*). Moreover, final recovery of proinsulin-WT was greatly increased in cells with increased ERO1β expression (Fig. 8*B*). Thus, despite presence of a coexpressed MIDY mutant, in cells with increased expression of ERO1, coexpressed proinsulin-WT exhibited improved folding and decreased ERAD (Fig. 8), explaining its secretion rescue (Fig. 7).

DISCUSSION

Point mutations adjacent to the SP cleavage site of preproteins may impair SP cleavage (37–39) and downstream folding (40) and can cause ER stress and cytotoxicity (41). In this report, we have investigated the biological behaviors of preproinsulin-A(SP23)S and A(SP24)D. These mutants provide a window into understanding the earliest steps of insulin biosynthesis. Unfortunately for patients expressing A(SP24)D, a series of pathological events go well beyond the defect in SP cleavage with failure to provide the critical free NH_2-terminal phenylalanine-B1 (33), impairing oxidation of the natural insulin disulfide bonds and creating a miscleaved SP, resulting in the ER retention of both forms of the mutant protein, blocking in trans the coexpressed proinsulin-WT from the normal *INS* gene allele and thereby profoundly inhibiting β-cell insulin production as well as induction of ER stress. On the positive side, we have developed a therapeutic maneuver that may minimize the dominant-negative effects of MIDY mutants.

All available evidence suggests that A(SP23)S is cleaved with normal efficiency (Fig. 2*A* and *B*) and fidelity to generate authentic proinsulin (Fig. 1*B*) and insulin (Fig. 1*C*) with no net ER stress beyond that seen for preproinsulin-WT (Fig. 1*D*). As serine is the native residue in this position in chimpanzee (Fig. 1*A*) and is the site of polymorphic variation in humans (29), we propose that in

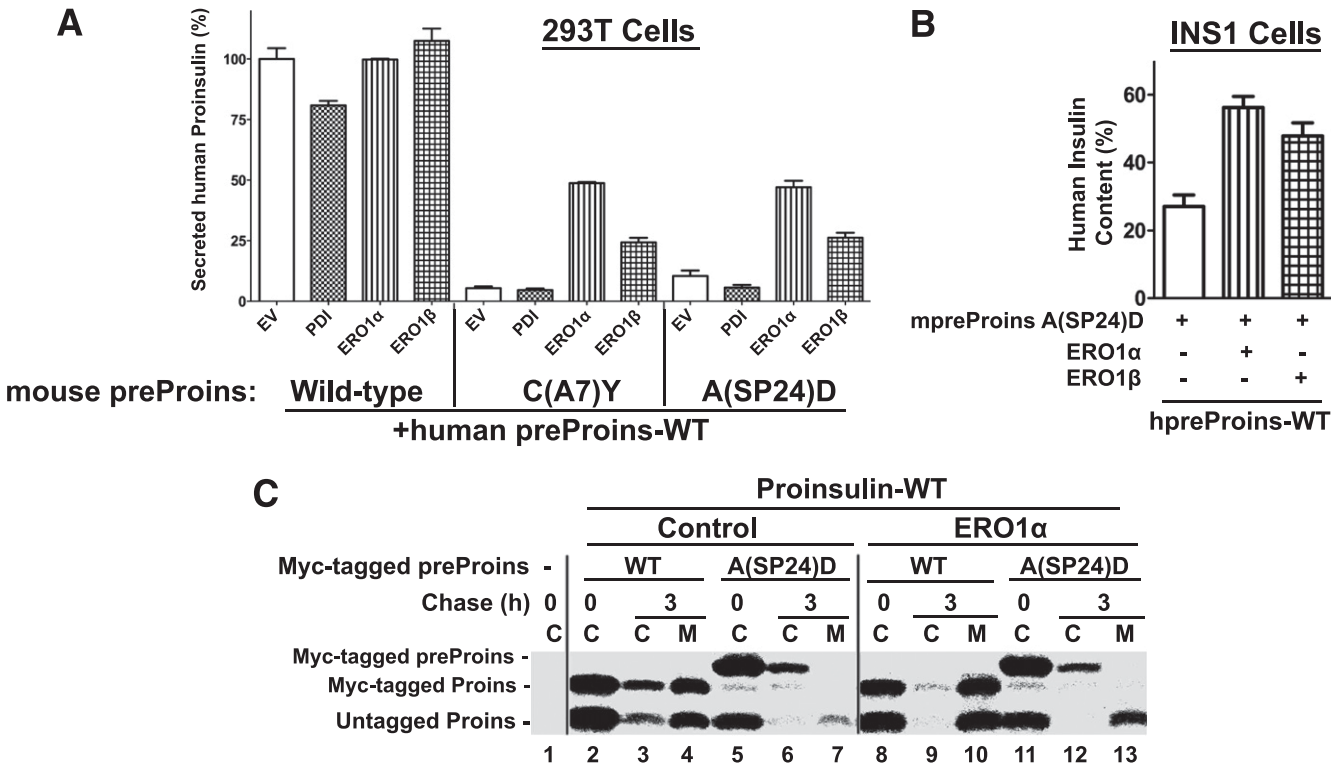

FIG. 7. Dominant-negative blockade of human proinsulin by A(SP24)D is partially rescued by increased expression of ERO1. *A*: At 48 h post-transfection, media bathing 293T cells coexpressing human preproinsulin-WT, one of the mouse preproins-[WT, C(A7)Y, or A(SP24)D], and empty vector (EV), PDI, or ERO1 (at a DNA molar ratio of 1:2:3) were collected for 16 h. Secreted human proinsulin was measured using a human-specific proinsulin RIA. Secretion of human proinsulin in the presence of mouse proinsulin-WT and empty vector was set to 100%. *B*: INS1 cells coexpressing human preproinsulin and mouse preproinsulin-A(SP24)D plus ERO1α or ERO1β (at a DNA molar ratio of 1:3:4) were lysed with acid/ethanol to measure human insulin content using human-specific insulin RIA. The human insulin content of cells cotransfected with WT human and mouse preproinsulins was set to 100%. *C*: At 48 h posttransfection, 293T cells coexpressing preproinsulin-WT and either preProCpepMyc-WT (processed to Myc-tagged Proins) or preProCpepMyc-A(SP24)D (shown as Myc-tagged preProins) plus empty vector (Control) or ERO1α (at a DNA molar ratio of 1:2:3) were pulse-labeled with ^{35}S-Cys/Met for 30 min and chased for 0 or 3 h. Newly synthesized (pre)proinsulins from cell lysates (C) and chase media (M) were immunoprecipitated with anti-insulin, resolved by Tris-Tricine urea–SDS-PAGE under reducing conditions, and analyzed by autoradiography.

spite of our earlier report (12), impaired preproinsulin SP cleavage and proinsulin misfolding are not operative for this particular variant. We cannot exclude that A(SP23)S might cause diabetes through a different mechanism. By contrast, although A(SP24)D is successfully translocated across the ER membrane (Fig. 3), it is inefficiently processed at an inappropriate SP cleavage site, generating a small subpopulation of miscleaved AD-Proins molecules (Figs. 1, 2, and 5–7). Both uncleaved and miscleaved A(SP24)D are retained intracellularly (Fig. 2*A*) and undergo ERAD (Fig. 2*C*), suggesting that they are misfolded. Nevertheless, at steady state, a major subpopulation of uncleaved A(SP24)D (along with the smaller subpopulation of SP cleaved) molecules accumulates in the ER (Fig. 1*B*), activating an ER stress response (Fig. 1*D*).

The half-life of preproinsulin-WT is exceedingly short, making it technically difficult to follow uncleaved preproinsulin in live cells (Fig. 4*B*). Cleavage by signal peptidase generally requires that 60–80 amino acids of the nascent polypeptide are cotranslationally translocated (42), which represents most of the preproinsulin molecule. What the A(SP24)D demonstrates is that preproinsulin Cys residues can be exposed to the oxidative environment of the ER even before SP cleavage (Fig. 4). To our knowledge, this is the first study to directly examine oxidative folding of preproinsulin in the ER. Normally, uncleaved preproinsulin-WT is fully reduced, and, upon SP removal, proinsulin begins to quickly form both native and isomeric disulfide bonds (Fig. 4*A* and *B*). However, under conditions in which normal SP cleavage is interrupted [e.g., in A(SP24)D], uncleaved preproinsulin exhibits delayed and abnormal oxidative folding (Fig. 4*A* and *B*), causing the formation of disulfide-linked complexes (Fig. 4*C*), which also entraps coexpressed proinsulin-WT (Fig. 4*D*).

We have previously shown that acute ER stress is not itself sufficient to block export of coexpressed WT *INS* gene product (21). Moreover, recent studies indicate that in MIDY, insulin deficiency precedes a net loss of β-cells (22,23). In this report, we demonstrate that A(SP24)D blocks the export of coexpressed proinsulin-WT (Fig. 6) and thereby decreases insulin production (Figs. 6*A* and 7*B*, open bar), which may be sufficient to account for initiation of insulin deficiency in patients with MIDY. The evidence suggests that it is primarily the uncleaved preproinsulin subfraction rather than the minor misfolded AD-Proins subfraction (Fig. 6*D* and E) that drives the dominant-negative insulin secretory behavior in patients bearing A(SP24)D.

Studies in humans suggest that one fully functional *INS* gene allele may be sufficient to maintain normoglycemia (5). We therefore reasoned that rescuing proinsulin-WT from dominant-negative blockade might restore insulin production to rescue from diabetes in MIDY. With this in mind, we have made a first attempt at a molecular therapeutic approach to rescue proinsulin-WT export in the

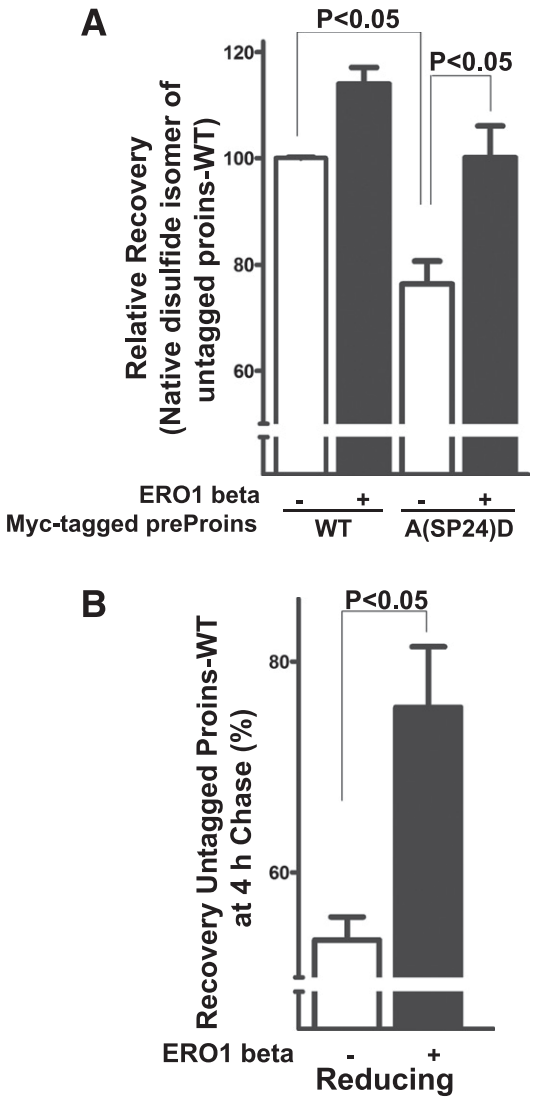

FIG. 8. Increased expression of ERO1β improves oxidative folding of proinsulin-WT in presence of A(SP24)D. *A*: At 48 h posttransfection, 293T cells coexpressing preproins-WT with Myc-tagged preproins-WT or -A(SP24)D, plus ERO1β (+) or empty vector (−) were pulse-labeled with ^{35}S-Cys/Met for 30 min without chase. The cells were lysed as in Fig. 4*A*, and coexpressed proins-WT was analyzed by immunoprecipitation and Tris-Tricine urea–SDS-PAGE under both nonreducing and reducing conditions, with quantitation by densitometry after autoradiography. The fractional recovery of the native disulfide isomer of untagged proins-WT under nonreducing conditions was compared against total proins-WT recovered under reducing conditions. The relative recovery of the native disulfide isomer of untagged proins-WT in the presence of Myc-tagged preproins-WT was set to 100% for purposes of comparison. *B*: Total newly synthesized proins-WT (from cell lysates plus chase media) recovered from immunoprecipitates analyzed by reducing Tris-Tricine urea–SDS-PAGE is shown over 4-h time course in the presence of coexpressed Myc-tagged preproins-A(SP24)D. Note that there was increased final recovery of total newly synthesized proins-WT in cells with increased expression of ERO1β.

presence of A(SP24)D; specifically searching for ways, without repairing the misfolding of MIDY mutants, that might enhance proinsulin-WT folding and ER export in order to limit its participation in aberrant protein complex formation in the ER (20). Formation of proinsulin's three disulfide bonds may occur via transfer of reducing equivalents to ER oxidoreductases and from there to the cytosol via ERO1; recently, Zito et al. (34) established that the diabetic phenotype of *Akita* mice is exacerbated upon loss of ERO1β. Conceivably, increased ERO1 or PDI expression might promote oxidative folding of proinsulin-WT. However, whereas increased PDI expression has been found to diminish glucose-stimulated insulin secretion and induce ER stress with accumulation of proinsulin in the ER (36), increased ERO1 expression promotes proinsulin-WT export through the secretory pathway (Fig. 7*A* and *C*), increasing insulin production (Fig. 7*B*). The simplest explanation for the increased insulin production is enhancement of oxidative folding of proinsulin-WT (Fig. 8*A*), decreasing its participation in disulfide-linked complexes (Fig. 8*A*), decreasing its ERAD (Fig. 8*B*), and increasing export of proinsulin-WT from the ER (Fig. 7).

Little progress has been made in the development of treatments for ER stress-related pancreatic β-cell failure. The ideas developed in this report suggest that enhancing the oxidative folding and export of proinsulin-WT may be a feasible way to restore insulin production in heterozygous MIDY patients. Several laboratories around the world have been working on small molecules that can manipulate the level and/or activity of ERO1β, and this may be a useful way forward. Moreover, it will be important to further explore the ratio of misfolded to total proinsulin forms, to understand the threshold of misfolding that is needed to trigger onset of insulin-deficiency and diabetes (23), and the means to raise that threshold by protecting bystander proinsulin export for insulin production and glucose homeostasis.

ACKNOWLEDGMENTS

This work was supported primarily by National Institutes of Health (NIH) grants R01-DK-48280 (to P.A.) and R01-DK-088856 and by March of Dimes 6-FY11-357 (to M.L.) as well as National Nature Science Foundation of China Grant 81070629 (to M.L.). We also acknowledge assistance from the Molecular Biology and DNA Sequencing Core of the NIH-funded Diabetes Research and Training Center (P60-DK-20572).

No potential conflicts of interest relevant to this article were reported.

M.L., R.L.-L., J.W., L.H., H.G., and D.L. researched data. M.L., S.-o.S., J.W., L.H., F.B., and P.A. contributed to discussion. M.L. and P.A. wrote the manuscript. M.L., J.W., F.B., and P.A. reviewed and edited the manuscript. P.A. is the guarantor of this work and, as such, had full access to all of the data in the study and takes responsibility for the integrity of the data and the accuracy of the data analysis.

The authors thank Bill and Dee Brehm for helping to create the Brehm Center for Diabetes Research to advance diabetes research at the University of Michigan.

REFERENCES

1. Hattersley A, Bruining J, Shield J, Njolstad P, Donaghue KC. The diagnosis and management of monogenic diabetes in children and adolescents. Pediatr Diabetes 2009;10(Suppl 12):33–42
2. Greeley SA, Tucker SE, Worrell HI, Skowron KB, Bell GI, Philipson LH. Update in neonatal diabetes. Curr Opin Endocrinol Diabetes Obes 2010;17:13–19
3. Fajans SS, Bell GI. MODY: history, genetics, pathophysiology, and clinical decision making. Diabetes Care 2011;34:1878–1884
4. Nishi M, Nanjo K. [The molecular mechanism of insulin biosynthesis and mutant insulin gene syndrome]. Nihon Rinsho 1994;52:2519–2527
5. Garin I, Edghill EL, Akerman I, et al; Neonatal Diabetes International Group. Recessive mutations in the INS gene result in neonatal diabetes through reduced insulin biosynthesis. Proc Natl Acad Sci USA 2010;107:3105–3110

6. Støy J, Edghill EL, Flanagan SE, et al; Neonatal Diabetes International Collaborative Group. Insulin gene mutations as a cause of permanent neonatal diabetes. Proc Natl Acad Sci USA 2007;104:15040–15044
7. Polak M, Dechaume A, Cavé H, et al; French ND (Neonatal Diabetes) Study Group. Heterozygous missense mutations in the insulin gene are linked to permanent diabetes appearing in the neonatal period or in early infancy: a report from the French ND (Neonatal Diabetes) Study Group. Diabetes 2008;57:1115–1119
8. Colombo C, Porzio O, Liu M, et al; Early Onset Diabetes Study Group of the Italian Society of Pediatric Endocrinology and Diabetes (SIEDP). Seven mutations in the human insulin gene linked to permanent neonatal/infancy-onset diabetes mellitus. J Clin Invest 2008;118:2148–2156
9. Ahamed A, Unnikrishnan AG, Pendsey SS, et al. Permanent neonatal diabetes mellitus due to a C96Y heterozygous mutation in the insulin gene. A case report. JOP 2008;9:715–718
10. Edghill EL, Flanagan SE, Patch AM, et al; Neonatal Diabetes International Collaborative Group. Insulin mutation screening in 1,044 patients with diabetes: mutations in the INS gene are a common cause of neonatal diabetes but a rare cause of diabetes diagnosed in childhood or adulthood. Diabetes 2008;57:1034–1042
11. Molven A, Ringdal M, Nordbø AM, et al; Norwegian Childhood Diabetes Study Group. Mutations in the insulin gene can cause MODY and autoantibody-negative type 1 diabetes. Diabetes 2008;57:1131–1135
12. Bonfanti R, Colombo C, Nocerino V, et al. Insulin gene mutations as cause of diabetes in children negative for five type 1 diabetes autoantibodies. Diabetes Care 2009;32:123–125
13. Rubio-Cabezas O, Edghill EL, Argente J, Hattersley AT. Testing for monogenic diabetes among children and adolescents with antibody-negative clinically defined Type 1 diabetes. Diabet Med 2009;26:1070–1074
14. Boesgaard TW, Pruhova S, Andersson EA, et al. Further evidence that mutations in INS can be a rare cause of Maturity-Onset Diabetes of the Young (MODY). BMC Med Genet 2010;11:42
15. Meur G, Simon A, Harun N, et al. Insulin gene mutations resulting in early-onset diabetes: marked differences in clinical presentation, metabolic status, and pathogenic effect through endoplasmic reticulum retention. Diabetes 2010;59:653–661
16. Liu M, Ramos-Castañeda J, Arvan P. Role of the connecting peptide in insulin biosynthesis. J Biol Chem 2003;278:14798–14805
17. Zhang BY, Liu M, Arvan P. Behavior in the eukaryotic secretory pathway of insulin-containing fusion proteins and single-chain insulins bearing various B-chain mutations. J Biol Chem 2003;278:3687–3693
18. Liu M, Li Y, Cavener D, Arvan P. Proinsulin disulfide maturation and misfolding in the endoplasmic reticulum. J Biol Chem 2005;280:13209–13212
19. Park SY, Ye H, Steiner DF, Bell GI. Mutant proinsulin proteins associated with neonatal diabetes are retained in the endoplasmic reticulum and not efficiently secreted. Biochem Biophys Res Commun 2010;391:1449–1454
20. Liu M, Hodish I, Rhodes CJ, Arvan P. Proinsulin maturation, misfolding, and proteotoxicity. Proc Natl Acad Sci USA 2007;104:15841–15846
21. Liu M, Haataja L, Wright J, et al. Mutant INS-gene induced diabetes of youth: proinsulin cysteine residues impose dominant-negative inhibition on wild-type proinsulin transport. PLoS ONE 2010;5:e13333
22. Gupta S, McGrath B, Cavener DR. PERK (EIF2AK3) regulates proinsulin trafficking and quality control in the secretory pathway. Diabetes 2010;59:1937–1947
23. Hodish I, Absood A, Liu L, et al. In vivo misfolding of proinsulin below the threshold of frank diabetes. Diabetes 2011;60:2092–2101
24. Hodish I, Liu M, Rajpal G, et al. Misfolded proinsulin affects bystander proinsulin in neonatal diabetes. J Biol Chem 2010;285:685–694
25. Liu M, Hodish I, Haataja L, et al. Proinsulin misfolding and diabetes: mutant INS gene-induced diabetes of youth. Trends Endocrinol Metab 2010;21:652–659
26. Sohma Y, Hua QX, Liu M, et al. Contribution of residue B5 to the folding and function of insulin and IGF-I: constraints and fine-tuning in the evolution of a protein family. J Biol Chem 2010;285:5040–5055
27. Rajan S, Eames SC, Park SY, et al. In vitro processing and secretion of mutant insulin proteins that cause permanent neonatal diabetes. Am J Physiol Endocrinol Metab 2010;298:E403–E410
28. Steiner DF, Chan SJ, Welsh JM, Kwok SC. Structure and evolution of the insulin gene. Annu Rev Genet 1985;19:463–484
29. Oda N, Nakai A, Fujiwara K, et al. Polymorphisms of the insulin gene among Japanese subjects. Metabolism 2001;50:631–634
30. Prehn S, Tsamaloukas A, Rapoport TA. Demonstration of specific receptors of the rough endoplasmic membrane for the signal sequence of carp preproinsulin. Eur J Biochem 1980;107:185–195
31. Miyamoto K, Yamashita T, Tsukiyama T, et al. Reversible membrane permeabilization of mammalian cells treated with digitonin and its use for inducing nuclear reprogramming by Xenopus egg extracts. Cloning Stem Cells 2008;10:535–542
32. Eskridge EM, Shields D. The NH2 terminus of preproinsulin directs the translocation and glycosylation of a bacterial cytoplasmic protein by mammalian microsomal membranes. J Cell Biol 1986;103:2263–2272
33. Liu M, Hua QX, Hu SQ, et al. Deciphering the hidden informational content of protein sequences: foldability of proinsulin hinges on a flexible arm that is dispensable in the mature hormone. J Biol Chem 2010;285:30989–31001
34. Zito E, Chin KT, Blais J, Harding HP, Ron D. ERO1-beta, a pancreas-specific disulfide oxidase, promotes insulin biogenesis and glucose homeostasis. J Cell Biol 2010;188:821–832
35. Khoo C, Yang J, Rajpal G, Wang Y, Liu J, Arvan P, Stoffers DA. Endoplasmic reticulum oxidoreductase-1-like {beta} (ERO1l{beta}) regulates susceptibility to endoplasmic reticulum stress and is induced by insulin flux in {beta}-cells. Endocrinology 2011;152:2599–2608
36. Zhang L, Lai E, Teodoro T, Volchuk A. GRP78, but not protein-disulfide isomerase, partially reverses hyperglycemia-induced inhibition of insulin synthesis and secretion in pancreatic {beta}-cells. J Biol Chem 2009;284:5289–5298
37. Nothwehr SF, Gordon JI. Structural features in the NH2-terminal region of a model eukaryotic signal peptide influence the site of its cleavage by signal peptidase. J Biol Chem 1990;265:17202–17208
38. Racchi M, Watzke HH, High KA, Lively MO. Human coagulation factor X deficiency caused by a mutant signal peptide that blocks cleavage by signal peptidase but not targeting and translocation to the endoplasmic reticulum. J Biol Chem 1993;268:5735–5740
39. Lyko F, Martoglio B, Jungnickel B, Rapoport TA, Dobberstein B. Signal sequence processing in rough microsomes. J Biol Chem 1995;270:19873–19878
40. Beuret N, Rutishauser J, Bider MD, Spiess M. Mechanism of endoplasmic reticulum retention of mutant vasopressin precursor caused by a signal peptide truncation associated with diabetes insipidus. J Biol Chem 1999;274:18965–18972
41. Kang SW, Rane NS, Kim SJ, Garrison JL, Taunton J, Hegde RS. Substrate-specific translocational attenuation during ER stress defines a pre-emptive quality control pathway. Cell 2006;127:999–1013
42. Eskridge EM, Shields D. Cell-free processing and segregation of insulin precursors. J Biol Chem 1983;258:11487–11491